ISSN 1392–3730 print / ISSN 1822–3605 online
**JOURNAL OF CIVIL ENGINEERING AND MANAGEMENT**
http:/www.jcem.vgtu.lt
*2006, Vol XII, No 2, 143–151*

# THE WOOD-FRAMED WITH SHEATHING BUILDINGS – ALTERNATIVE FOR HOUSING CONSTRUCTION

**Mikołaj Malesza, Czesław Miedziałowski**
*Dept of Civil Engineering, Białystok University of Technology ul. Wiejska 45E, 15-351 Białystok, Poland. E-mail: m.malesza@wp.pl*

*Received 26 July 2005; accepted 05 Oct 2005*

**Abstract.** Numerical model of the wood-framed with sheathing structure and selected results of experimental tests are presented in the paper. Wall and floor diaphragms as the three-dimensional composite structure are modelled applying plane shell elements representing framing and sheathing and beam element describing the fasteners. Experimental tests were conducted on typically disposed the wood-framed wall and floor diaphragms in residential housing in Poland. Associated tests of materials and connections and their results are also included in the paper. Non-linear behaviour of fasteners is examined in the numerical model. Results obtained from model and experiments are coincident.

**Keywords:** wood-framed structure, numerical model, load-slip characteristic, wall displacements, stud and sheathing stressing, non-linearity of structure.

## 1. Introduction

A significant number of residential buildings in Poland and in Central Europe countries is constructed of the wood framed with a sheathing technology. North-eastern part of Poland, Lithuania and Scandinavia are covered with the biggest forest complexes still existing in Europe. Therefore this method of housing construction implemented with a new technology of manufacturing creates a progressive future for building industry. Compared to the former traditional in Poland in the past technology of the solid wood die square walls, the wood-framed buildings require a low volume of lumber. Solid wood is used in construction of the walls, floors and roof diaphragms (studs, floor joints, roof rafters and girders). Lateral stiffness of diaphragms is achieved applying plywood, chipboards or other structural board of sheathing to the timber frame.

Fasteners linking sheathing to the wooden frame and diaphragms interconnecting links redistribute loading of structural elements, and they are affecting the lateral strength and displacements of building [1, 2]. A layer of mineral wool placed between studs and joists supplemented outside of the wall diaphragms satisfies the predicted conditions of thermal and acoustic requirements [3].

The paper presents examples of construction, selected results of experimental tests and analytical modelling as well as investigations of the wood-framed with sheathing buildings.

## 2. Construction

The building under construction and a typical cross-section of the wall and floor or roof diaphragms are presented in Fig 1.

Wood-framed with sheathing buildings are actually constructed in Poland by a prefabricated large-panel technology. This technology requires a well-equipped plant, much know-how of technical and working staff and management acting on the domestic and foreign building market. The quality of final product in respect of construction, finishes and time-table must be guarantied the in hard reality of market requirements. High quality and precise design technique are required to avoid exceeding the overstressing of the inter-element connection and the cross-section bearing capacity. Fig 2 presents the way of large panel manufacturing and the assembly on the site.

Advanced research works are conducted abroad [4, 5]. These works are concentrated on improving the building structure and introduction of analytical models predicting the structure static and dynamic behaviour [6, 7].

Experimental testing, analytical investigations and practical implementations of the wood-framed with sheathing buildings are conducted for 15 years at the Bialystok Technical University [8–10].

Mechanics of internal forces redistribution, evaluation of interaction of structural elements, prediction of displacements in the three-dimensional scheme are the topic of these works.

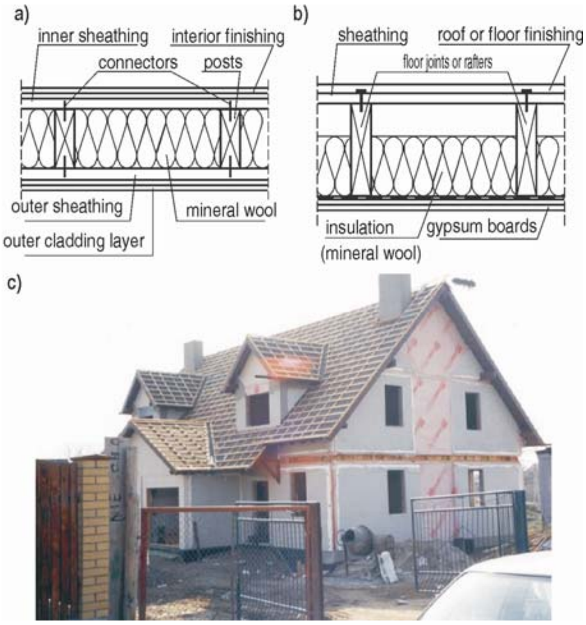


**Fig 1.** Typical cross-section of the wood-framed structures and a building under construction: a) wall diaphragms, b) floor and roof panel, c) a building under construction

**Fig 2.** Manufacture plant and assembly on the site: a) manufacture plant, b) assembly on the site

Results of experimental tests are compared with some analytical predictions obtained applying the numerical and analytical models.

## 3. Experimental tests

Six different geometry wall diaphragms were tested experimentally. The full and perforated wall panels one side sheathed with the dimension of 2750x3750 mm are presented in Fig 3.

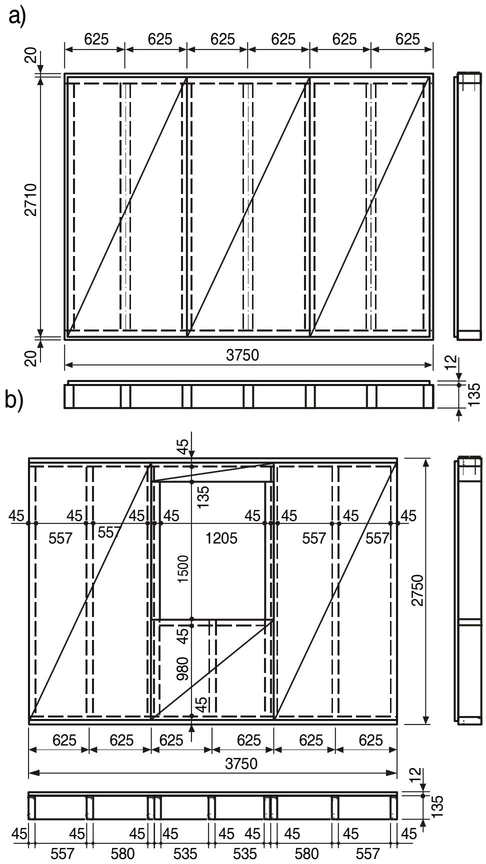


**Fig 3.** Experimentally investigated wall panels:
a) full wall panel A, b) perforated wall panel B

Spruce wood-framing, wood derivative sheathing boards and nail fasteners were used in wall panel construction. Dimensions of panel and material were selected from usual construction elements of the wood-framed residential housing. Framing consisting of 45x135 mm cross-section studs, horizontal top and bottom plates of 45x135 mm were constructed using class C27 solid wood. One-side sheathing thickness of 12,5 mm chipboard V100 class was applied to the framing using nailing G2.7/65 mm along the perimeter of the board distanced on 150 mm, and 300 mm on the intermediate studs of the framing. Wooden framing posts and the horizontal plates were connected by two nails G5.0/150 mm to each post. In case of perforated walls, window opening dimension of 1205x1500 mm was located in the middle part of diaphragm.

The lintel of the cross-section 3x45x135 mm supported by two additional posts was placed above the opening. Additional horizontal plate (45x135 mm) and intermediate post were placed under the window opening.

Experimental tests of wall diaphragms were conducted according to the procedure of European Standard EN 594.

The vertical and horizontal loading was applied using the hydraulic coupled-system of operators. The loading phases and their scheme of application are presented in Fig 4.

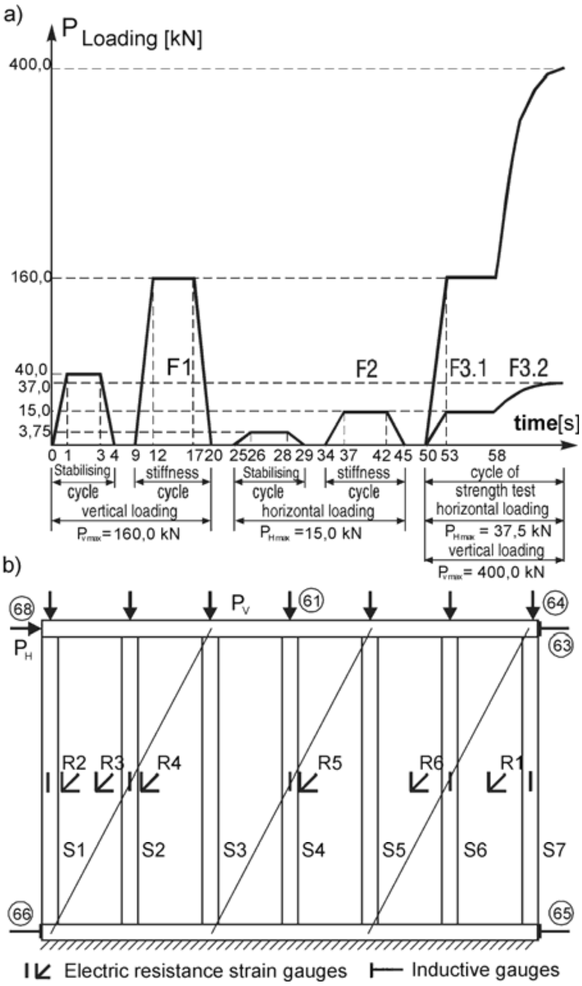


**Fig 4.** Scheme of application and phases of loading: a) phases of loading, b) strain gauges and inductive gauges location

The following phases of loading in experimental tests of panels according to PrEN 594 were selected:

- stabilising 1 (vertical loading F1) under concentrated load of Pv0 = 0,1 $P_v$, where $P_v$ = 400 kN for wall A without opening and $P_v$ = 250 kN for perforated wall B,
- functional live loading F1 (vertical loading F1) under concentrated load of $P_{v1}$ = 0,4 $P_v$,
- stabilising 2 (horizontal loading F2) under concentrated horizontal load of $P_{Ho}$ = 0,1 $P_H$, where $P_H$ = 37,5 kN for wall A and $P_H$ = 25,0 kN for wall B,
- functional horizontal load (horizontal loading F2) under concentrated load of $P_{H2}$ = 0,2 $P_H$,
- simultaneous vertical and horizontal loading F3 up to the failure of tested elements presented in Fig 4a.

Strains were measured by electric resistance strain gauges and displacements of the tested diaphragms were read off from the inductive gauges. Location of the reading places is shown in Fig 4b. Sheathing to framing connectors were tested according to Standards of EN383 and corresponding PN-EN 26891 "Joint made with mechanical fasteners – General principles for the determination of strength and deformation characteristics", in the range of theirs strength and deformability C. Behaviour of fastener and surrounding material response presents Fig 5.

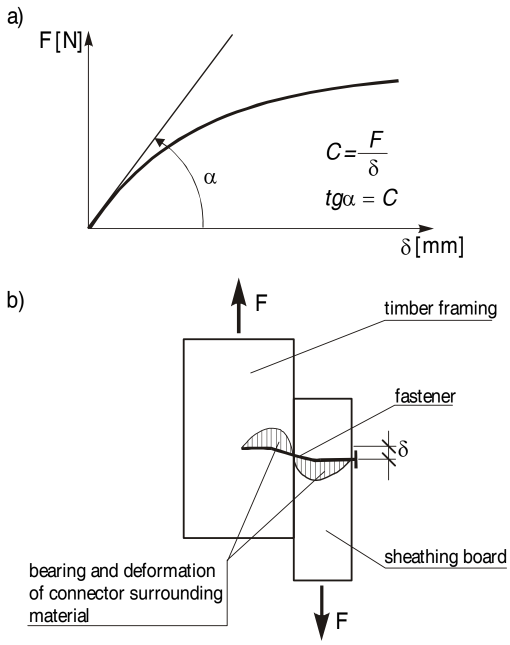


**Fig 5.** Behaviour of fastener and response of surrounding material: a) load-slip characteristic, b) behaviour of fastener surrounding material

Basic characteristics of material properties for wood and chipboards and their modulus of elasticity (MOE) were also experimentally investigated. Materials characteristics are set in Table 1.

## 4. Analytical models

### 4.1. Standards approach

Different standards are based on two methods of analysis of the wood-framed elements [11–13]. The first procedure is based on prediction of design load of diaphragm from the analogy parameters obtained from experimental tests of the standard test elements [11].

The designed lateral load of the diaphragm is computed from the formula:

$$F_{Ki} = k_b \cdot k_h \cdot F_{test,k} \,, \qquad (1)$$

where: $k_b = f(b_i, b_{test})$ for $b_i$ and $b_{test}$ – the length of designed panel and tested wall, angle of rotation of the strip cross-section,

$k_h = f_1(h_i, h_{test})$ for $h_i$ and $h_{test}$ – the height of designed panel and tested correspondingly,

$F_{test,k}$ – characteristic lateral load of tested wall diaphragm dimensions $b_{test}$ x $h_{test}$,

$F_{ki}$ – characteristic lateral load of the wall diaphragm dimension $b_i$ x $h_i$.

The other way is based on analytically calculated lateral bearing capacity of the wall diaphragm on the base of designed lateral load of single fastener linking sheathing to framing [11] according to formula:

$$F_{v,d} = \sum R_d \left(\frac{b_i}{b_1}\right)^2 \frac{b_i}{s} \,, \qquad (2)$$

where: $R_d$ – designed lateral load of fastener,

$b_i$ – the width of the sheathing boards,

$b_1$ – the width of the widest sheathing boards,

$s$ – spacing of fasteners along the perimeter of sheathing boards.

Compressed and tensioned studs are designed under loading

$$F_{ci} = \alpha_i \cdot F_{v,d} \frac{h_i}{b_i} \,, \qquad (3)$$

$$F_{ti} = F_{v,d} \cdot \frac{h_i}{b_i} \qquad (4)$$

added from to the axial load in studs from vertical loadings.

The standard [12] is based on minimum lateral load obtained from experimental tests for different kind of sheathing having introduced various factors influencing the designed wall lateral load [12].

These standards are based on formula:

$$F_{v,d} = F_{d_{tests}} \cap K_i \,, \qquad (5)$$

where: $F_{d,test}$ – basic racking resistance for certain materials and combination of materials obtained from the test of wall diaphragm 2,40 m square,

$K_i$ – the modification factors contributing: size of fasteners, their spacing, sheathing boards thickness, height of the wall, length of wall, window, door and other fully framed openings in wall, variation in vertical load.

Redistribution of externally applied loading to the wall diaphragm among all elements of framing and sheathing is based on two procedures as well.

The first procedure compares the external load to the evaluated by the experimental test of similar wall panel results.

The second method leads to the distribution of externally acting on the diaphragm load to each stud and sheathing of the parts of panel without openings.

The diagram of distribution of internal forces within the diaphragm is presented in Fig 6.

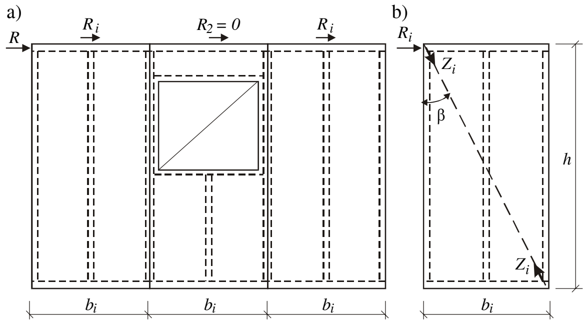


**Fig 6.** Distribution of internal forces within diaphragm: a) lateral load distributed in the wall, b) lateral load distributed within the single panel

The internal forces are computed by formulas

$$C_i = \alpha_i \cdot \frac{R_i \cdot h}{b_i} \,, \qquad (6)$$

$$T_i = \frac{R_i \cdot h}{b_i} \,, \qquad (7)$$

$$Z_i = \frac{R_i \cdot h}{b_i \cdot sin\alpha} \,, \qquad (8)$$

where: $R_i$ – the lateral load to the full segment of wall,

$h$ – height of wall diaphragm,

$b$ – width of panel.

### 4.2. Numerical model

Development of higher computer abilities and new numerical approach begin the application of advanced analytical and numerical methods based on truss analogy using the finite element method.

The analytical model proposed by the authors and based on the finite element method for wall diaphragms (full or perforated) is presented in Fig 7.

Detailed discretisation of sheathing to framing connection details of lintels remains the important part of numerical model. Fig 8 presents selected details of discretisation used in the numerical model.

Four nodes shell finite element describe wooden framing and sheathing. The shell and beam finite elements are used in the presented physical models of diaphragms approximate applying the finite element methods (FEM). The analytical model is built on the basis of the FEM utilising locally formulated element stiffness matrices and loading vector. The plate and plane stress elements constituted the shell element used in description of analytical model are shown in Fig 9. Displacements in that way formulated shell state of loading are described by vector:

$$\mathbf{u} = \{u, v, w, \varphi_x, \varphi_y, \varphi_z\}. \qquad (9)$$

Considering separately the state of plane stress and the state of plate stress, the displacements and loading vectors are obtained:

$$\mathbf{u}^{\mathrm{t}} = \{\, \mathrm{u}, \mathrm{v} \} \,, \qquad (10)$$

$$\mathbf{W}^{\mathrm{t}} = \{\, N_x, N_y \} \,. \qquad (11)$$

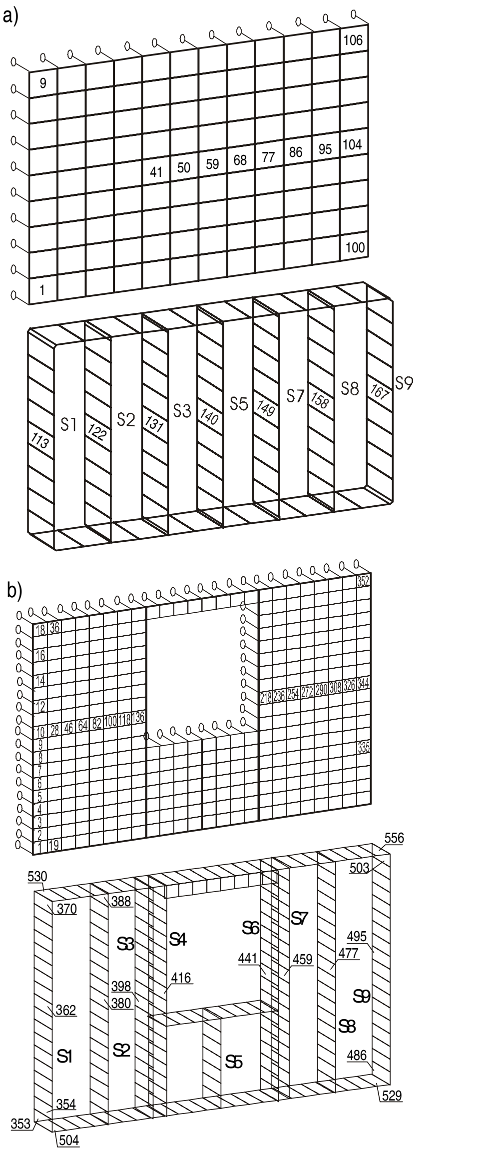


Fig 7. Wall element discretisation: a) full segment of diaphragm discretisation, b) perforated wall diaphragm discretisation

The strain vector on the basis of the plane state of stress has the form:

$$\boldsymbol{\varepsilon}^{t}=\begin{Bmatrix}\varepsilon_x\\ \varepsilon_y\\ \gamma_{xy}\end{Bmatrix}=\begin{bmatrix}\dfrac{\partial}{\partial x} & 0\\ 0 & \dfrac{\partial}{\partial x}\\ \dfrac{\partial}{\partial y} & \dfrac{\partial}{\partial y}\end{bmatrix}\begin{Bmatrix}u\\ v\end{Bmatrix}=\mathbf{L}^{t}\mathbf{u}^{t}. \quad (12)$$

Matrix of the finite element nodal displacements has the form

$$\mathbf{d}_{e}^{t}=\left\{u_1,v_1,u_2,v_2,u_3,v_3\right\}. \quad (13)$$

The stiffness matrix is obtained from typical relations of the finite element method in the form

$$\mathbf{K}_{e}^{t}=\int_{\Omega}\mathbf{B}_{t}^{T}\mathbf{D}_{t}\mathbf{B}_{t}\, d\Omega, \quad (14)$$

where $B_t$ – strain matrix for plane state of stress in the form

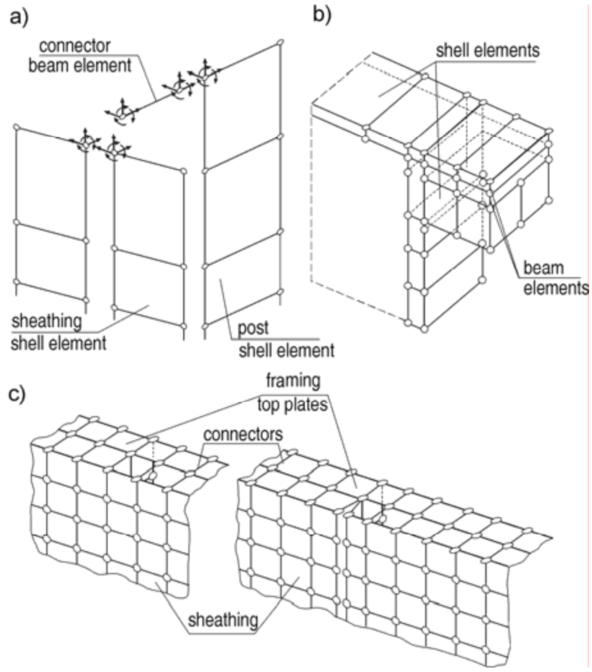


Fig 8. Details of discretisation: a) sheathing to framing connection with fastener, b) modelling of lintel, c) two boards of sheathing applied to the framing

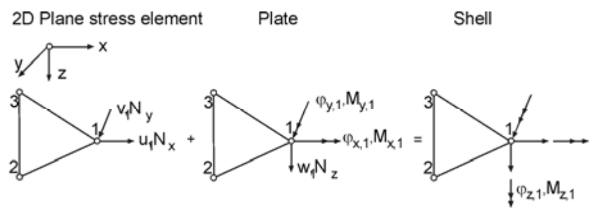


Fig 9. The sum of triangles creating the shell element

$$\mathbf{B}_{t}=\mathbf{L}^{t}\mathbf{N}^{t}, \quad (15)$$

for $N^t$ – the shape function matrix for plane state and $D^t$ – constitutive matrix for isotropic or orthotropic material.

In case of the plate state it is obtained

$$\mathbf{u}^{P}=\left\{w,\varphi_x,\varphi_y\right\}, \quad (16)$$

$$\mathbf{W}^{P}=\left\{N_z,M_x,M_y\right\}. \quad (17)$$

The strain vector has the form

$$\varepsilon^{P}=\begin{Bmatrix}\varepsilon_x\\ \varepsilon_y\\ \gamma_{xy}\end{Bmatrix}=-z\begin{Bmatrix}\dfrac{\partial^2}{\partial x^2}\\ \dfrac{\partial^2}{\partial y^2}\\ 2\dfrac{\partial^2}{\partial x\,\partial y}\end{Bmatrix}w=-z\,\mathbf{L}^{p}\,w. \quad (18)$$

Nodal displacements of finite elements can be described in the form

$$\mathbf{d}_{e}^{P}=\left\{w_1,\varphi_{x1},\varphi_{y1},w_2,\varphi_{x2},\varphi_{y2},w_3,\varphi_{x3},\varphi_{y3}\right\}. (19)$$

The stiffness matrix of the plate element is computed in a similar way and it has the form

$$\mathbf{K}_e^P = \int_\Omega \mathbf{B}_p^T \overline{\mathbf{D}}_p \mathbf{B}_p \, d\Omega, \tag{20}$$

$$\mathbf{B}_P = \mathbf{L}^P \mathbf{N}^P, \tag{21}$$

where $\overline{\mathbf{D}}_P$ – constitutive matrix for the plate state, $N^P$ – the shape function for the plate state.

The sum of plate and 2D state of stress elements parameters leads to the elimination parameters in z direction; torsion moment $M_z$ and $\varphi$ angle of rotation incomplete in the $z$ direction may develop some singularities of the stiffness matrix.

Inadequate rotational stiffness of joint in the $z$ direction also incorporates some physical uncertainties. The so-called fictitious torsion stiffness for perpendicular to element axis is introduced in order to eliminate that irregularity resulted from the following dependence:

$$\begin{Bmatrix} M_{z1} \\ M_{z2} \\ M_{z3} \end{Bmatrix} = \begin{bmatrix} k_{11}^s & k_{12}^s & k_{13}^s \\ k_{21}^s & k_{22}^s & k_{23}^s \\ k_{31}^s & k_{32}^s & k_{33}^s \end{bmatrix} \begin{Bmatrix} \varphi_{z1} \\ \varphi_{z2} \\ \varphi_{z3} \end{Bmatrix} = \mathbf{K}_e^s \varphi_{zi} \,. \tag{22}$$

Matrix $\mathbf{K}_{es}$ elements are selected for moments $M_{zi}$ equal to zero and equal values of $\varphi_{zi}$ angles.

The plain triangular shell element in local coordination system has the symmetric stiffness matrix 18x18 elements and originates by overlapping the sub matrices $\mathbf{K}_e^t$, $\mathbf{K}_e^P$ and $\mathbf{K}_e^s$. As a result of four triangular elements linking in one node, quadrilateral five nodal elements are created. The interior node can be then eliminated by static condensation and four nodal elements obtained as a result.

Connecting sheathing to framing fasteners is described by applying finite beam elements with parameters obtained from experimental tests. Both sheathing and framing materials surround and respond to fastener slip-displacements.

From the experimental test of the connector load-slip characteristic the stiffness is obtained by the formula

$$C = \frac{F}{\delta}, \tag{23}$$

here: $C$ – modulus of fastener deformability,

$F$ – lateral load on fastener,

$\delta$ – slip on joint.

By the mechanics the theoretic displacement of both sides the fixed beam under bending and shear is computed using the formula

$$\delta = \frac{Fl^3}{12\,EI}\left(1 + \frac{12\,EI\,\alpha}{l^2 GA}\right), \tag{24}$$

where: $A$, $I$ – substitute cross-section characteristics of fastener,

$l$ – the length of fastener,

$\alpha = \frac{10}{9}$ – parameter of circle cross-section.

Comparing (23) and (24) formulas, the reduced stiffness of the finite beam element is obtained:

$$\mathbf{D} = \left\{ EA, {GA}/{k_y}, {GA}/{k_z}, EI_y, EI_z, GI_s \right\}. \tag{25}$$

Displacements of the beam element axis is described in the form

$$\mathbf{u} = \{u, v, w, \varphi_y, \varphi_z, \varphi_s\} \tag{26}$$

and strain as

$$\boldsymbol{\varepsilon} = \{\varepsilon, \beta_y, \beta_z, \chi_y, \chi_z, \chi_s\}. \tag{27}$$

The matrix form of strain-displacements relations for beam element is described as

$$\boldsymbol{\varepsilon} = \mathbf{Lu}, \tag{28}$$

where $\mathbf{L}$ – the matrix of differential operators.

Internal forces are computed by formula

$$\mathbf{W} = \mathbf{DLu}, \tag{29}$$

where $\mathbf{W} = \{N_1, T_y, T_z, M_y, M_z, M_s\}$.

Applying the finite element method, the unknown compounds of nodal displacements vector have the form

$$\mathbf{d}_e = \{u^i, v^i, w^i, \varphi_y^i, \varphi_z^i, \varphi_s^i, u^k, v^k, w^k, \varphi_y^k, \varphi_z^k, \varphi_s^k\}. \tag{30}$$

Typical procedures of the finite element method lead to the stiffness matrix of the fastener

$$\mathbf{K}_e = \int_l \mathbf{B}^T \mathbf{D} \mathbf{B} \, dz, \tag{31}$$

where $\mathbf{B}$ – strain matrix;

$\mathbf{B} = \mathbf{LN}$ for;

$\mathbf{N}$ – the shape function matrix.

Analytical model of the wall diaphragm is built from shell and beam finite element describing framing, sheathing and fasteners and equation system describing equilibrium. It has the form

$$\mathbf{Kd} = \mathbf{P}. \tag{32}$$

Strong non-linear behaviour of the sheathing to framing fastener is noticed during the test. The stiffness of structure depends on stressing the elements and equilibrium equations are obtained in non-linear form

$$\mathbf{K}(d)\mathbf{d} = \mathbf{P}. \tag{33}$$

The global stiffness matrix depends on the phase of loading and stiffness of fastener (linking sheathing to framing) is strongly varying. Unchanged geometry of fastener and its diameter $d$ and $l$ – length lead to modulus $E$ varying in the form

$$E_i = C_i \cdot \gamma = C_o \cdot \gamma \cdot \left(\frac{C_i}{C_o}\right), \tag{34}$$

where

$$C_o = \lim_{\delta \to 0} \frac{F(0+\delta)}{\delta}; \; C_i = \frac{F_i}{\delta_i} \tag{35}$$

and

$$\gamma = \frac{l^3}{12\,I}\left[1 + 0{,}75(1+\nu) \cdot \alpha \left(\frac{d}{l}\right)^2\right]. \tag{36}$$

The superelements technique is adopted in formulating three-dimensional numerical model of building structure. 3D superelements modulating building structure is presented in Fig 10.

The stiffness matrices component structural building elements wall diaphragm, floor slabs, roof are created providing their interconnection and the applied way of loading transmission.

Interconnections of wall floor and roof diaphragms in the three-dimensional model of building structure are presented in Fig 10.

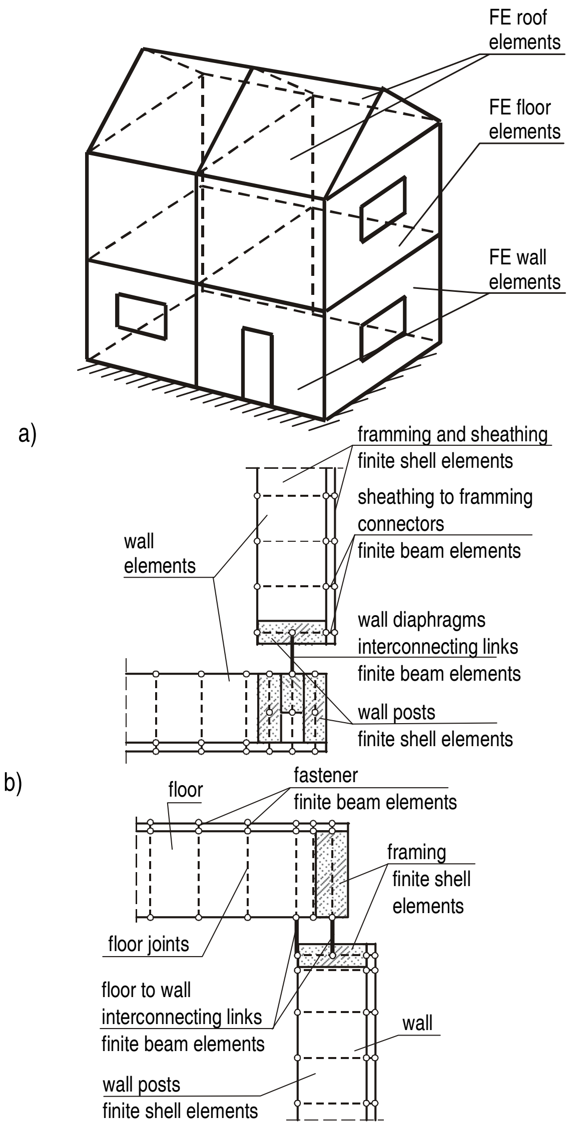


**Fig 10.** Modelling the building and joints a) walls at the corner, b) floor to wall

Superelements stiffness matrices are created as a result of the equilibrium equations system segregation in following way

$$\begin{bmatrix} \mathbf{K}_{11} & \mathbf{K}_{12} \\ \mathbf{K}_{21} & \mathbf{K}_{22} \end{bmatrix} \begin{bmatrix} \mathbf{u}_1 \\ \mathbf{u}_2 \end{bmatrix} = \begin{bmatrix} \mathbf{P}_1 \\ \mathbf{P}_2 \end{bmatrix}, \quad (37)$$

where: $\mathbf{K}_{ij}$ – block of matrices assigned to appropriate the groups of unknowns,

$\mathbf{u}_1$ – nodal displacements vector at the border and interconnecting the superelements,

$\mathbf{u}_2$ – displacements vector internal elements,

$\mathbf{P}_1$, $\mathbf{P}_2$ – loading of internal and external nodes.

As a result of conversion considering $u_2$ displacement, the equation has the form

$$\left[\mathbf{K}_{11} - \mathbf{K}_{12}(\mathbf{K}_{22})^{-1}\mathbf{K}_{21}\right]\mathbf{u}_1 = \mathbf{P} - \mathbf{K}_{12}(\mathbf{K}_{22})^{-1}\mathbf{P}_2 \quad (38)$$

or the simplified formula

$$\mathbf{K}^s\mathbf{u}^s = \mathbf{P}^s, \quad (39)$$

where: $\mathbf{K}^s$ – superelement stiffness matrix,

$\mathbf{u}^s = \mathbf{u}^1$ – superelement unknown displacements vector,

$\mathbf{P}^s$ – superelement loading vector.

Analytical-numerical model of the three-dimensional whole building structure is built introducing global coordinates system and numeration according to formula

$$\mathbf{K} = \sum_{re}\sum_{e}\mathbf{K}^s, \quad \mathbf{u} = \sum_{re}\sum_{e}\mathbf{u}^s, \quad \mathbf{P} = \sum_{re}\sum_{e}\mathbf{P}^s, \quad (40)$$

where: $re$ – type of superelements; wall, floor and roof diaphragms,

$e$ – sequent elements in type.

## 5. Results and analyses

Table 1 presents the selected results of tests of material characteristics.

**Table 1.** Material characteristics

| Material | $E_{11}$ [MPa] | $E_{22}$ [MPa] | G [MPa] | $V_{12}$ | $V_{21}$ |
|---|---|---|---|---|---|
| Wood | 11 500 | 530 | 585 | 0,3690 | 0,0341 |
| Plywood | 10 900 | 8 700 | 790 | 0,1740 | 0,0380 |
| Chipboard | 4 500 | 3 800 | 800 | 0,1640 | 0,2430 |
| Gypsum board | 3 900 | 3 500 | 1 800 | 0,1062 | 0,1636 |

Load-slip characteristics of sheathing to framing connections are presented in Fig 11.

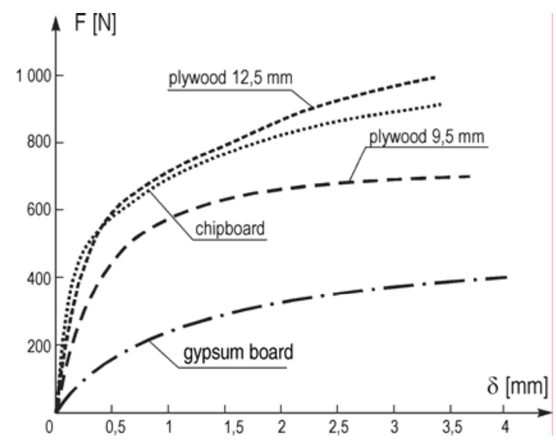


**Fig 11.** Deformability of sheathing to framing connectors for different sheathing material

Applying the least-square method the best fitted curve describing fastener behaviour has been selected:

$$F = (A + B\delta)\left(1 - e^{-\frac{C}{A}\delta}\right), \tag{41}$$

where parameters $A$, $B$, $C$ were obtained from the results of tests for different sheathing material used in construction. $A$, $B$, $C$ parameters are set in Table 2.

**Table 2.** Parameters of the load-slip characteristics

| Parameters sheathing material | Plywood 12,5 mm | Plywood 9,5 mm | Chipboard 12,5 mm | Gypsum board 12,5 mm |
|---|---|---|---|---|
| A | 0,597 | 0,587 | 0,600 | 0,315 |
| B | 114,72 | 29,13 | 100,91 | 17,96 |
| C | 3 491,76 | 1 557,50 | 2 498,93 | 421,10 |

Fig 10 shows a strong non-linearity of sheathing to framing connector behaviour.

The load-displacement characteristics $P = f(\delta)$ of the wall diaphragms without openings obtained from experimental test and received in results of analysis applying the proposed numerical model is presented in Fig 12.

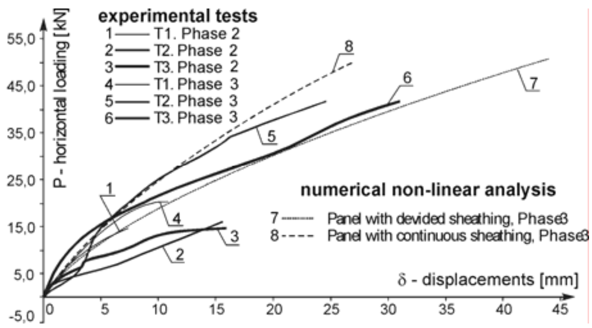


**Fig 12.** Experimental and analytical characteristics of wall deformability

Also non-linearity of wall diaphragm behaviour is evident. Critical deformations were observed at the edge located fasteners connecting sheathing to framing. Those fasteners commence the process of diaphragm failure as a result of sheathing disintegration from framing and connector yielding.

External load applied to the wall diaphragm is transferred to each element of the combined structure. For different stages of loading the stress in studs and sheathing were obtained by experiment and numerical approach.

The stress at the mid-height of the studs under F.3.1 phase of loading obtained by experiment and compared to analytical-numerical analysis are set in Table 3 and presented in Fig 13.

The stress distribution in the sheathing across the section at the mid-height of the diaphragm is also computed in similar way utilising the numerical model and then compared with experimental test results. Stressing in the sheathing is conditioned by the properties of material in respect of diaphragm static work of wall.

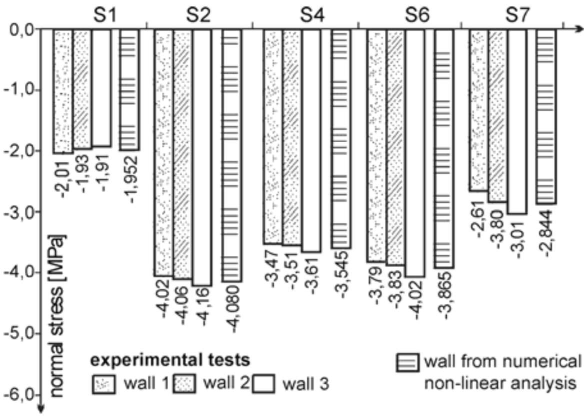


**Fig 13.** Diagram of stressing in the studs of walls without opening

**Table 3.** Normal stress in the sheathing

| Lp | Tested sheathing element | Normal stress $\sigma_y$ [MPa] from experimental tests T1 | T2 | T3 | from non-linear numerical analyses T1 | T2 | T3 | Stage of loading |
|---|---|---|---|---|---|---|---|---|
| 1 | R2 | -0,41 | -0,34 | -0,39 | -0,39 | | | F1 Pv = 160,91 kN |
| 2 | R3 | -0,40 | -0,43 | -0,38 | -0,37 | | | |
| 3 | R4 | -0,37 | -0,33 | -0,36 | -0,36 | | | |
| 4 | R5 | -0,42 | -0,36 | -0,41 | -0,40 | | | |
| 5 | R6 | -0,40 | -0,49 | -0,38 | -0,36 | | | |
| 6 | R1 | -0,39 | -0,50 | -0,40 | -0,34 | | | |
| 7 | R2 | 0,72 | 0,67 | 0,63 | 0,70 | | | F2 $P_H$ = 15,00 kN |
| 8 | R3 | 0,32 | 0,22 | 0,26 | 0,30 | | | |
| 9 | R4 | -0,06 | -0,05 | -0,08 | -0,04 | | | |
| 10 | R5 | -0,17 | -0,15 | -0,18 | -0,14 | | | |
| 11 | R6 | 0,07 | 0,04 | 0,08 | 0,04 | | | |
| 12 | R1 | -0,80 | -0,75 | -0,79 | -0,74 | | | |
| 13 | R2 | 0,31 | 0,35 | -0,37 | 0,35 | | | F3.1 $P_v$ = 153,80 kN $P_H$ = 14,40 kN |
| 14 | R3 | 0,00 | 0,01 | 0,02 | 0,00 | | | |
| 15 | R4 | -0,22 | -0,30 | -0,35 | -0,31 | | | |
| 16 | R5 | -0,47 | -0,52 | -0,55 | -0,52 | | | |
| 17 | R6 | -0,22 | -0,20 | -0,24 | -0,23 | | | |
| 18 | R1 | -0,99 | -1,03 | -1,17 | -1,08 | | | |
| 19 | R2 | 0,47 | 1,18 | 2,49 | 0,46 | 1,16 | 2,48 | F3.2* |
| 20 | R3 | -0,11 | 0,20 | 0,67 | -0,10 | 0,18 | 0,69 | |
| 21 | R4 | -0,62 | -0,72 | -0,90 | -0,62 | -0,71 | -0,91 | |
| 22 | R5 | -0,94 | -1,10 | -1,29 | -0,94 | -1,07 | -1,29 | |
| 23 | R6 | -0,38 | -0,14 | -0,34 | -0,38 | -0,13 | -0,33 | |
| 24 | R1 | -1,96 | -2,81 | -4,28 | -1,96 | -2,78 | -4,28 | |

* Panel T1 $P_v$ = 344,70 kN $P_H$ = 21,38 kN
Panel T2 $P_v$ = 351,99 kN $P_H$ = 52,23 kN
Panel T3 $P_v$ = 354,08 kN $P_H$ = 52,23 kN

## 6. Conclusions

- The paper presents analyses of the internal forces redistribution in the composite wood-framed wall diaphragms under combined vertical and horizontal loading.
- Wall diaphragm behaviour under lateral and vertical load results of experimental tests and on the base of the elaborated numerical model.
- Effects of redistribution of internal forces in three-dimensional wood-framed structure

strongly depend on the fastener linking sheathing to framing and its stiffness.

- Non-linearity of the sheathing to framing fastener remains the main source of the wall diaphragm non-linear behaviour.
- Results obtained from the numerical model for 3D wall diaphragm match with good similarity the experimental tests results in the range of displacements and stress distribution.

## References


1. Hite, M. C. and Shenton, I. H. Modelling of the non-linear behaviour of wood frame shear walls. In: Proc of 15th ASCE Engineering Mechanics Conference, June 2-5, 2002, Columbia University, New York, 2002, p. 1–8.
2. Robertson, A. and Griffits, R. Factors affecting the racking resistance of timber frame panels. *Journal of the Institution of Structural Engineering*, Vol 59B, No 4, 1981, p. 49–63.
3. Malesza, M. and Miedziałowski, Cz. Performance and design of low energy consuming the light wood framed residential buildings in Poland. In: Proc of 5th International Conference: Modern Building Materials, Structures and Techniques, Vilnius, May 21–24, 1997. Vilnius: Technika, 1997, p. 214–219.
4. Tissel, J. R. Wood structural panel shear walls. Research Report No 154, American Plywood Association, May 1993. 18 p.
5. Tissel, J. R. and Elliott, J. R. Plywood diaphragms. Research Report No 138, American Plywood Association, Sept 1999. 55 p.
6. Kasal, B. and Leichti, R. J. Nonlinear finite element model of light-frame wood structures. *Journal of Structural Engineering*, Vol 120, No 12, 1994, p. 100–119.
7. Schmidt, R. J. and Moody, R. C. Modeling lateraly loaded light-frame buildings. *Journal of Structural Engineering*, Vol 115, No 1, 1989, p. 201–217.
8. Malesza, M. and Miedziałowski, Cz. Experimental test of wood-framed buildings wall. *Engineering and Building* (Inżynieria i Budownictwo), No 4, 1999, p. 208–210 (in Polish).
9. Malesza, M. and Miedziałowski, Cz. Application of quasi-shell elements in analysis of three-dimensional wood-framed sheathed structures. In: Proc of 4th International Colloquium on Computation of Shell & Spatial Structures IASS-IACM 2000, Chania, Crete, Greece, 4–7 June 2000, p. 402–403.
10. Malesza, M. and Miedziałowski, Cz. Discrete analytical models of wood-framed with sheathing buildings structures and selected experimental test resultants. *Archives of Civil Engineering*, Vol XLIX, Issue 2, 2003, p. 213–240.
11. PN-B-03150:2000. Polish Standard. Timber structures – calculation and design rules. (Konstrukcje drewniane - obliczenia statyczne i projektowanie). Polish Committee for Standardization, Warsaw, Poland, 2000. 96 p. (in Polish).
12. BS 5268: Part 6: Section 6.1:1988. British Standard. Structural use of timber. Code of practice for timber frame walls. Dwellings not exceeding three storeys. British Standards Institute, London, UK, 1988. 22 p.
13. DIN 1052: 2004. German Standard. Design of timber structures - general rules and rules for buildings. (Entwurf, Berechnung und Bemessung von Holzbauwerken - allgemeine Bemessungsregeln und Bemessungsregeln für den Hochbau). German Institute for Standardization, Berlin, 2004. 34 p. (in German).


## APKALTINIAI MEDKARKASIŲ KONSTRUKCIJŲ PASTATAI – ALTERNATYVA NAMŲ STATYBAI

**M. Malesza ir C. Miedziałowski**


S a n t r a u k a

Straipsnyje pateiktas apkaltinės medkarkasio konstrukcijos skaitinis modelis bei atrinkti eksperimentinių bandymų rezultatai. Sienų ir perdangų diafragmos modeliuotos kaip erdvinė kompozitinė konstrukcija naudojant lėkštus kevalinius elementus, atitinkančius sienos karkasą ir apkalą, bei sijinį elementą, atitinkantį junges. Eksperimentiniai bandymai vykdyti su Lenkijoje tipiškų gyvenamųjų namų mediniu strypynu, sienų ir perdangų diafragmomis. Straipsnyje taip pat pateikti kartu vykdytų medžiagų bei jungčių bandymai ir jų rezultatai. Jungių netiesinė elgsena nagrinėta remiantis skaitiniu modeliu. Iš modelio ir eksperimentų gauti rezultatai yra tapatūs.


**Reikšminiai žodžiai:** medinio strypyno konstrukcija, skaitinis modelis, apkrovos ir slinkties charakteristika, sienos poslinkiai, statramsčių ir apkalos įtempiai, konstrukcijos netiesiškumas.


**Czesław MIEDZIAŁOWSKI.** Dept of Civil Engineering, Białystok University of Technology, ul. Wiejska 45E, 15-351 Białystok, Poland. Ph, fax: 048 085 7422413.

E-mail: *cz.miedzialowski@kmb.pb.bialystok.pl*


Professor of strength of materials and mechanics of structure at the Building Engineering Institute of the Technical University of Bialystok, Poland. His research interests include modelling the structures applying numerical methods.

**Mikołaj MALESZA**. Dept of Civil Engineering, Białystok University of Technology, ul. Wiejska 45E, 15-351 Białystok, Poland. Ph, fax: 048 085 7422413. E-mail: m.malesza@wp.pl, corresponding author

Reader in timber and masonry structures at the Building Engineering Institute of the Technical University of Bialystok, Poland. His research interests include the non-linear behaviour of the wood-framed structural elements and the effect of duration of load on connections slip.